Adoptive transfer of CX3CR1 transduced-T regulatory cells improves homing to the atherosclerotic plaques and dampens atherosclerosis progression

Short title: Engineered Treg therapy for atherosclerosis

F. Bonacina[1], E. Martini[2], M. Svecla[1], J. Nour[1], M. Cremonesi[2], G. Beretta[3], A. Moregola[1], F. Pellegatta[4], V. Zampoleri[1,5], A.L. Catapano[1,4], M. Kallikourdis[2,6*], G.D. Norata[1,5*]

[1]Department of Excellence of Pharmacological and Biomolecular Sciences, Università degli Studi di Milano, Milan, Italy; [2]Adaptive Immunity Lab, Humanitas Clinical and Research Center, Rozzano - IRCSS, Italy; [3] Department of Environmental Science and Policy, Università degli Studi di Milano; [4]IRCSS Multimedica, Milan, Italy; [5]Centro SISA per lo Studio dell'Aterosclerosi, Ospedale Bassini, Cinisello Balsamo, Italy; [6]Humanitas University, Pieve Emanuele, Italy.

*Co-last authors

§Corresponding authors:

Prof. Giuseppe Danilo Norata, Department of Excellence of Pharmacological and Biomolecular Sciences, University of Milan. Via Balzaretti 9, 20133, Milan, Italy.

Prof. Alberico Luigi Catapano, Department of Excellence of Pharmacological and Biomolecular Sciences, University of Milan. Via Balzaretti 9, 20133, Milan, Italy

E-mail: Danilo.Norata@unimi.it

Total word count: 8397

Original Article

1. Abstract

Aim: Loss of immunosuppressive response supports inflammation during atherosclerosis. We tested whether adoptive cell therapy (ACT) with Tregulatory cells (Tregs) engineered to selectively migrate in the atherosclerotic plaque would dampen the immune-inflammatory response in the arterial wall in animal models of Familial Hypercholesterolemia (FH).

Methods and Results: FH patients presented a decreased Tregs suppressive function associated to an increased inflammatory burden. A similar phenotype was observed in *Ldlr -/-* mice accompanied by a selective increased expression of the chemokine CX3CL1 in the aorta but not in other districts (lymph nodes, spleen and liver). Treg overexpressing CX3CR1 were thus generated ($CX3CR1^+$-Treg) to drive Treg selectively to the plaque. $CX3CR1^+$-Treg were injected (i.v.) in *Ldlr -/-* fed high-cholesterol diet (WTD) for 8 weeks. $CX3CR1^+$-Treg were detected in the aorta, but not in other tissues, of *Ldlr -/-* mice 24h after ACT, corroborating the efficacy of this approach. After 4 additional weeks of WTD, ACT with $CX3CR1^+$-Treg resulted in reduced plaque progression and lipid deposition, ameliorated plaque stability by increasing collagen and smooth muscle cells content, while decreasing the number of pro-inflammatory macrophages. Shotgun proteomics of the aorta showed a metabolic rewiring in $CX3CR1^+$-Treg treated *Ldlr -/-* mice compared to controls that was associated with the improvement of inflammation-resolving pathways and disease progression.

Conclusion: ACT with vasculotropic Treg appears as a promising strategy to selectively target immune activation in the atherosclerotic plaque.

Keywords: Tregulatory cells – cellular therapy - atherosclerosis

2. Translational relevance

Improving pro-resolutive inflammatory response represents a promising therapeutic approach to control atherosclerosis progression. Meanwhile, selective immunosuppression at the atherosclerotic plaque looks critical to limit unspecific inhibition of inflammation in other tissues. Our work demonstrates that engineering of immunosuppressive T regulatory cells to be hijacked in the atherosclerotic plaque limits atherosclerosis progression by targeting local inflammation.

3. Introduction

Elevated levels of cholesterol and apolipoprotein B containing lipoproteins represent a causal factor for atherosclerosis. In patients with Familial Hypercholesterolemia (FH), impaired LDL-C clearance [1, 2] results in hypercholesterolemia followed by cholesterol deposition in the arteries as well as in the skin, thus causing extensive xanthoma formation, and premature and progressive atherosclerotic disease [3]. Hypercholesterolemia promotes also an extensive immune-inflammatory response in the atherosclerotic plaque [4], which results from an increased immune activation coupled to defective inflammation-resolving mechanisms [5], including impaired surveillance by Tregulatory cells (Tregs). Tregs play a critical role in the maintenance of immune homeostasis and prevention of autoimmunity [6] and, in the context of atherosclerosis, promote plaque stability by suppressing pro-inflammatory lymphocytes, via secretion of anti-inflammatory molecules (including IL-10 and TGFβ) [7-9] and by promoting macrophage efferocytosis [10]. While alterations in circulating levels of Tregs not always mark atherosclerosis [11-14], reduced numbers of Tregs were detected in vulnerable plaques compared to stable plaques [15], and in experimental models Treg deficiency was shown to promote atherosclerosis progression. Therefore, different strategies based on Tregs have been tested to dampen atherosclerosis progression, including Treg adoptive cell transfer (ACT) [16, 17], in vivo Treg expansion by IL-2/IL-2 antibody complexes [18], or Treg induction by tolerogenic dendritic cells exposed to relevant atherosclerosis-related antigens [19-21].

The translation of these approaches in the context of cardiovascular atherosclerotic diseases, in spite of promising findings, however has been limited so far by i) potentially deleterious off-target immunosuppression induced by the systemic Treg increase, ii) non-selective cell expansion, thus driving the concomitant activation of other immune cells beyond Tregs, or iii) the challenge to identify suitable antigens to induce a robust protection against atherosclerosis [22, 23].

We therefore hypothesized that strategies able to improve Treg homing to the atherosclerotic lesions would help to overcome these limitations and result in plaque-selective dampening of the immunoinflammatory response. Selective chemokine/chemokine receptor crosstalk has been used to control tumour growth by

forcing effector T cell recruitment to cancer tissues [24, 25]. Therefore, we decided to engineer Tregs to express the chemokine receptor that matched those chemokines selectively expressed in the atherosclerotic plaque and explored selective homing and efficacy of engineered Treg on atherosclerosis in experimental models. To this aim we first profiled chemokines expressed in atherosclerotic plaques of *Ldlr -/-* mice and identified fractalkine (CX3CL1) as a specific chemokine expressed in the atherosclerotic plaque but not in other tissues. Treatment with CX3CR1^{+}-engineered Treg resulted in preferential homing to the plaque, where they reduced the atherosclerotic lesion and improved plaque stability in *Ldlr -/-* mice. Aortic shotgun proteomics showed that engineered Treg promoted plaque stability and reduced inflammatory burden, as revealed by increased collagen deposition, smooth muscle cell content and improved efferocytosis.

4. Methods

4.1 Human samples

Patients with genetic diagnosis of Familial Hypercholesterolemia were recruited to the Centre for the study of Atherosclerosis at Bassini Hospital (Cinisello Balsamo, Italy) within the Lipigen study, an integrated network aimed at improving the identification of patients with genetic dyslipidaemias, including FH, in Italy [26]. Further information is available in **Supplemental Material** and clinical characteristics are presented in **Supplemental Table 1.** The study was approved by the Ethical Committee of IRCCS Multimedica "LIPIGEN - LIpid TransPort Disorders Italian GEnetic Network – Italian Registry of Familial Dyslipidemias (N.13/2011/Cardiovascolare).

All participants signed an informed consent in accordance with the Declaration of Helsinki.

4.2 Mice

Wild type and *Ldlr -/-* male mice on C57BL/6J background were purchased from The Jackson Laboratory (USA). Mice were housed four per cage and kept in a temperature-controlled environment (20 ± 2°C, 50 ± 5% relative humidity) with a 12-hour light/dark cycle and free access to food and water. All animal procedures performed conformed to the guidelines from 2010/63/EU directive of the European Parliament on the protection of animals used for scientific purposes and were approved by the Ethical Committee (Progetto di Ricerca 2012/02).

6-8 weeks old mice were fed a high cholesterol diet (western type diet - WTD, E15775-34 ssniff® Spezialdiäten GmbH, DE) for 8-12 weeks, depending on experimental conditions (details are reported in the text and figure legends). For ACT, mice were anesthetized with ketamine/xylazine (15 mg/Kg + 10 mg/Kg respectively, i.p.) and Treg injected retro-orbitally and randomly allocated to experimental groups. For tissue collection, mice were euthanised by an overdose of CO_2.

4.3 Quantitative real time PCR (qRT-PCR)

For chemokine expression analysis, aortas, mediastinal lymph nodes, livers, spleens and inguinal lymph nodes were homogenized with Tissue Lyser II (QIAGEN) and total RNA was extracted using RNeasy Mini Kit (Qiagen).

The same amount of RNA was retrotranscribed using High Capacity cDNA Reverse Transcription kit (Applied Biosystems). Real-time qPCR reactions were performed using TaqMan Probes and TaqMan Universal Master Mix on a ViiA7 (ThermoFisher) instrument. Please see the **Major Resources Table** in the **Supplemental Materials** for additional information.

4.4 Flow cytometry

Immunophenotyping was performed on blood (100 µL for human, 50 µL for mice) or cell suspensions (from lymph nodes, spleen and aorta). Blood was incubated at RT for 30 minutes with the specific antibody mixture and thereafter samples were lysed and fixed (eBioscience) according to manufacturer instructions. Single cell suspensions were incubated with antibody mixtures at 4°C for 30 minutes and then washed with PBS/FBS 2%/EDTA 2mM. For intracellular staining, first cells were fixed and permeabilized (eBioscience) according to manufacturer instructions then incubated with specific antibodies at 4°C for 30 minutes. Samples were acquired with Novocyte 3000 (ACEA Biosciences) and analysed with Novoexpress software (ACEA Bioscience). Antibodies used are listed in the **Supplemental Table 2** and the different gating strategies are presented in Supplementary Figures.

Murine Treg purity and transduction efficiency were assessed on LSR Fortessa (BD) and analysed using FlowJo (9.9.6) software.

4.5 Isolation of $CD4^+$Tcells and Treg from human blood and murine lymphoid organs

Detailed protocols are described in **Supplemental Material.**

4.6 $CD4^+$T cells proliferation and cytokine production

PBMC from humans or lymphocyte suspension from murine lymphoid organs were stained with 3µM of CFSE (SIGMA-ALDRICH), incubated for 10 minutes at RT in dark, diluted 10 times in PBS/FBS 2%/2mM EDTA, washed 3 times and re-suspended in warm media. $2.5x10^5$ cells were plated with 200 µL of complete RPMI (Euroclone; plus 10% FBS, glutamine, HEPES, MeOH, sodium pyruvate and antibiotics, R10) in the presence of IL-2 (10U/mL, Peprotech) in 96-well plate (U-bottom wells) coated with 2µg/mL anti-CD3 (eBioscience) and 5

µg/mL CD28 (eBioscience) for 5 days at 37°C with 5% of CO_2. Proliferation was assessed by CFSE dilution by flow cytometry and calculated by mitotic index, defined as the ratio between the number of T cells undergoing mitosis to the total number of plated T cells. The index is calculated for each cell division from the sum of mitotic events adjusted for the number of cell precursors [27].

For cytokine production, after 5 days of culture, cells were pulsed with anti-CD3 (1 µg/mL, eBioscience) and CD28 (2.5 µg/mL, eBioscience) for 4 hours at 37°C with 5% of CO_2 in the presence of Brefeldin A (1:1000, BD Biosciences). Cytokine staining was performed by flow cytometry following the instructions from the fixation/permeabilization kit (BD Bioscience). Antibodies are listed in Supplementary Table 2.

4.7 Treg suppression assay

Purified CD4 T conventional cells ($CD4^+CD25^-$) were stained with CFSE (SIGMA-ALDRICH, Cat#21888), incubated for 10 minutes at RT in dark, diluted 10 times in PBS/FBS 2%/2mM EDTA, washed 3 times and re-suspended in warm media. $2.5x10^5$ cells were plated in the presence of increasing concentration of Treg cells ($CD4^+CD25^+$, ratio Tconv:Treg 1:0, 1:0.25, 1:0.5, 1:1) in 200 µL of complete RPMI (R10) in the presence of IL-2 (10U/mL, Peprotech) in 96-well plate (U-bottom wells) coated with 2µg/mL anti-CD3 (eBioscience) and 5 µg/mL CD28 (eBioscience) for 5 days at 37°C with 5% of CO_2. Suppression of $CD4^+CD25^-$ T cell proliferation was assessed by flow cytometry as the percentage of cells in proliferation, under each condition of Treg co-incubation (1:0.25, 1:0.5, 1:1), adjusted for their basal proliferation (1:0).

4.8 Treg transduction

To generate retroviral vectors, one day prior to transfection, $4x10^5$ HEK 293 T cells/well were plated into a 6-well plate in 2 ml of Iscove's Modified Dulbecco's Medium (IMDM) with high glucose L-glutamine, 0.001% 2-mercaptoethanol and 10% fetal calf serum, without antibiotics. Transient transfection of the HEK 293 T was performed in Optimem (Gibco) medium with 1.6% Lipofectamine 3000 (Invitrogen), 2 µg of packaging vector pCL-Eco (Imgenex) in combination with plasmid encoding for Green Fluorescent Protein (GFP) (m6p-egfp) (kind gift of Dr Randow and Dr Betz, MRC-LMB, Cambridge, UK) or m5p-CX3CR1-2A-EGFP. The next day, murine Treg were isolated with CD4+ CD25+ Regulatory T Cell Isolation Kit (Miltenyi). 48 and 72 hours post-

transfection, Treg cells were transduced by adding 1/3 volume filtered supernatants of the transfected HEK 293 T cells to the Treg cells, along with fresh IL-2 and a final concentration of 6μg/ml of protamine sulphate (Sigma Aldrich), after which cells were spun for 2 hours at 1800 rpm at 32°C. Transduction efficiency was assessed via FACS analysis.

4.9 Aorta processing for histology, immunofluorescence and flow cytometry analysis

Aorta freshly collected were fixed overnight in PBS/formaldehyde 3% (Merck) and included in paraffin for hematoxylin/eosin and Masson's Trichrome (Bio-Optica) stainings, and α-actin (Novus Biologicals), Mac-2 (Cedaelane) and *in situ* cell death detection (Merck) fluorescent stainings, or in OCT (Tissue-Tek, Sakura) for oil Red O'staining (Bio-Optica).

Additional details together with aorta digestion and staining for flow cytometry information are provided in Supplemental Material.

4.10 Proteomic analysis

Aorta segments from mice receiving the same treatment (n=4 *Ldlr -/-* mice treated with ctrl-Treg versus n=5 treated with CX3CR1^{+}-Treg) were pooled up to 20 mg and lysed in the presence of RIPA buffer (Tris-HCl 50 mM pH 7.2, EDTA 5 Mm, SDS 0.1%) and protease inhibitors (Cell Signaling) at a ratio of 1:100 and used for LC-MS/MS analysis.

Methodological details are provided in Supplementary Material.

4.11 Statistical analysis

Graph Pad-Prism8 was used for graphic presentation and statistical analysis. Results are given as the mean per group ± SEM. The data were analysed according to what reported in figure legends and a p-value of <0.05 was considered significant. For comparison between two groups unpaired two-sides T-test with a 95% confidence interval and parametric test was used assuming a gaussian distribution of data. For multiple comparisons, ANOVA test was applied. The qPCR data were analysed using the delta CT method by taking the CT values of the genes of interest from the housekeeping gene following by normalization to the wild type control sample.

Please see **Supplemental Material** for additional methodological details.

5. Results

5.1 T regulatory cells from patients with Familial Hypercholesterolaemia display impaired immunosuppressive function.

Immunophenotypic analysis of $CD4^+$ T cell subset distribution in subjects with genetic diagnosis of familial hypercholesterolemia (FH) (**Supplementary Table 1**) unveiled an increased frequency of circulating $CD4^+$ T effector memory cells ($CCR7^-CD45RA^-$) and a reduction of T central memory cells ($CCR7^+CD45RA^-$) compared to age and sex matched controls (**Figure 1A**). When challenged in vitro, $CD4^+$ T cells from FH patients showed a significative increase in cell proliferation compared to those from healthy controls (**Figure 1B**), paralleled by enhanced production of pro-inflammatory cytokines (IFNγ and TNFα) and reduced synthesis of IL-10 following cell activation (**Figure 1C**). To test whether this phenotype could depend on a defective immunosuppressive function of T regulatory cells (Treg), we analysed Treg levels, phenotype and function in FH patients. Although circulating Treg ($CD4^+CD127^{lo}CD25^{hi}$) frequency was increased in FH subjects (**Figure 1D**), Treg suppressive function toward conventional $CD4^+$ T ($CD4^+CD25^-$) proliferation was reduced as compared to Tregs from healthy controls (**Figure 1E**).

A similar profile was observed in *Ldlr -/-* mice (the experimental model mimicking the defect of familial hypercholesterolemia, **Supplementary Figure 2A**) which displayed increased proliferation of $CD4^+$ T cells (**Supplementary Figure 2B**) and increased frequency of circulating $FoxP3^+$ $CD4^+$ T cells (**Supplementary Figure 2C-2D**) compared to WT mice, a finding that is in agreement with previous gene expression studies performed on experimental model of atherosclerosis [12]. Similar to FH subjects, Tregs from *Ldlr -/-* mice showed a decreased suppressive function compared to those from WT mice (**Supplementary Figure 2E**). All together these data indicate that compromised Treg suppressive function contributes to the enhanced $CD4^+$ T response in FH patients, partly compensated by an increase in Treg circulating levels, a feedback mechanism already reported in patients affected by autoimmune diseases [12, 28].

5.2 CX3CR1/CX3CL1 axis defines atherosclerotic plaque targeting

These results set the stage for testing strategies aimed at improving Treg efficiency to dampen atherosclerosis progression in FH models. To overcome poor homing selectivity toward the atherosclerotic plaque and off-target immunosuppression and confine Treg immunosuppressive response to this site, we tested the possibility to drive Treg homing preferentially to the vascular lesion by inducing ectopic expression of the receptor matching chemokine specifically expressed in the atherosclerotic plaque. This approach was successfully used to vehiculate cytotoxic T cells to cancer tissues where they dampened tumour growth [24].

To this aim, we first profiled mRNA expression of a set of inflammatory cytokines involved in immune cells recruitment (CCL2, CCL5, CCL4, CXCL9, CXCL10, CXCL11 and CX3CL1) in the aorta, spleen, liver, mediastinal lymph nodes (those draining the heart and the aortic arch) and inguinal lymph nodes of *wild type* and *Ldlr -/-* mice after 8 weeks of high-cholesterol diet (WTD). CX3CL1 expression was significantly increased in the aorta of Ldlr -/- mice but not in other tissues compared to wild type controls (**Figure 2A-2B**), whereas among other chemokines previously described to play a critical role during atherogenesis, CCL2, although largely expressed in the atherosclerotic plaque of *Ldlr -/-* was also expressed in other tissues including lymph nodes and liver (**Figure 2A** and **Supplementary Figure 3A-3G**), thus implying a lower aortic selectivity compared to CX3CL1. Of note CCL4, CXCL11 and CXCL9 were increased mainly in lymph nodes but not in the aorta (**Figure 2A** and **Supplementary Figure 3A-3G**). These observations suggest that CX3CL1 could enable selective recruitment to the vessel wall in the context of atherosclerosis. In line with these observations, CX3CL1 plasma levels were significantly increased in *Ldlr -/-* mice compared to *wild type* (**Figure 2C**).

To further characterize the relevance of the CX3CL1/CX3CR1 axis, we evaluated CX3CR1 expression among different subsets of circulating immune cells in mice, showing that the receptor is largely expressed on monocytes ($Ly6C^+$ cells), but minimally expressed on $CD4^+$ or $CD8^+$ T cells (**Figure 2E and Supplementary Figure 3H**). These findings set the stage for testing whether ectopic expression of CX3CR1 on Treg cells could represent a strategy to selectively vehiculate Tregs to the atherosclerotic plaque and impact plaque development. Tregs were isolated from WT mice and then transfected with the IRES-EGFP vector coding for

CX3CR1 or with an empty vector (**Figure 3A**). Transfection, detected by GFP positivity, did not alter expression of CD25 compared to freshly isolated Tregs (**Supplementary Figure 4A**), in accordance with our previous data showing that this procedure maintains engineered Treg in vivo suppressive potential[29]; in addition, CX3CR1 receptor expression was clearly detectable on the surface of GFP^+ cells transduced with the CX3CR1 vector, compared to cells transfected with the empty vector (**Figure 3B**). Next, $CX3CR1^+$-Treg cells were tested in vivo for selective migration to the atherosclerotic aorta; $2x10^5$ GFP^+ Treg (ctrl and overexpressing CX3CR1) were i.v. injected in two months old *Ldlr -/-* mice fed for 8-weeks a WTD to induce atherosclerosis. Twenty-four hours after the injection, Treg homing in the aorta as well as in other tissues were assessed by flow cytometry (**Figure 3A, 3C** and **Supplementary Figure 4B-4D**). *Ldlr -/-* mice receiving CX3CR1+-Treg showed an increased frequency of GFP+ cells in the aorta compared to mice treated with ctrl-Treg, while the migration to other tissues, including mediastinal (those draining the aortic arch) and inguinal lymph nodes or spleen was similar in mice injected with ctrl- or CX3CR1+-Treg (**Supplementary Figure 4B-4D**), marking the distribution of injected cells after an adoptive cell transfer. These data indicate that ectopic expression of CX3CR1, selectively drives Treg to the aorta of atherosclerotic mice.

5.3 Engineered Tregs dampen atherosclerosis progression, improve atherosclerotic plaque stability and efferocytotic response.

To evaluated whether adoptive cell therapy with engineered Tregs ($CX3CR1^+$) impacts on atherosclerosis progression, two months old *Ldlr -/-* mice were fed WTD for 8-weeks and then received ACT with ctrl- or $CX3CR1^+$-Treg and fed WTD for 4 additional weeks (**Figure 4A**). At the end of the treatment, GFP^+ were still detected in the atherosclerotic aorta of mice receiving $CX3CR1^+$-Tregs ACT (**Figure 4B**), paralleled by few cells still detectable in the circulation, while no GFP^+ Treg cells were detected in the mediastinal lymph nodes (**Supplementary Figure 5A**). No differences were observed in the levels of endogenous Tregs among the different groups (**Supplementary Figure 5B**). Most importantly, the treatment with $CX3CR1^+$-Tregs resulted in a significant reduction of plaque area at the aortic sinus compared to ctrl-Tregs (99658±11782 μm^2 vs 65016±9446 μm^2; **Figure 4C**, **4G**). Of note, mice treated with ctrl-Tregs presented a plaque area similar to that of untreated *Ldlr -/-* (**Supplementary Figure 5C**). Treatment with $CX3CR1^+$-Tregs resulted also in reduced

necrotic core (14362±5161 vs 6586±1401 μm^2; p=0.07 **Figure 4D**), a significant increase in collagen content (24,50%±2,27% vs 30,67%±1,43%; **Figure 4E**, **4G**) and a significant reduction in lipid deposition (38,94%±1,595% vs 34,39%±0,96%; **Figure 4F**, **4G**) compared to mice treated with ctrl-Tregs. These data demonstrated that adoptive cell transfer with CX3CR1$^+$-Tregs reduced atherosclerosis progression and improved plaque phenotype. This effect was independent of major changes in circulating plasma lipid levels (cholesterol and triglycerides) (**Supplementary Figure 5D**), or in immune cells phenotype in the circulation (neutrophils, monocytes, T cells and their subsets, **Supplementary Figure 6A**) and mediastinal lymph nodes (T cells, **Supplementary Figure 6B**).

To further investigate the impact of engineered Treg adoptive therapy on atherosclerotic plaque characteristics, shotgun proteomics was performed on aortic samples of ctrl- or CX3CR1$^+$-Treg treated *Ldlr -/-* mice (**Supplementary Figure 7A**). Out of 1174 proteins detected, 340 were differently regulated, with mice treated with CX3CR1$^+$-Treg presenting 152 proteins upregulated and 190 proteins downregulated compared to ctrl-Treg treated mice (**Figure 5A** and **Supplementary Figure 7B**). Principal components analysis (PCA) and proteins expression profile clearly identified a different signature in the aorta of *Ldlr -/-* mice treated with CX3CR1$^+$-Treg compared to those treated with ctrl-Treg (**Figure 5B-5C**). Up- and down-regulated proteins were then categorized based on gene ontology (GO) analysis in biological processes, cellular components and molecular functions (**Supplementary Figure 7C**); network analysis highlighted proteins related to pathways associated to inflammation, cellular metabolism and energy production as well as extracellular matrix biology that emerged as significantly modulated by CX3CR1$^+$-Treg treatment (**Figure 5D**). Biological pathway analysis based on z-score revealed that proteins associated with extracellular matrix organization, such as endothelial cell and fibroblast migration, actin filament organization and integrin signalling were upregulated in Ldlr -/- mice treated with CX3CR1$^+$-Treg compared to those treated with ctrl-Treg (**Figure 6A**). CX3CR1$^+$-Treg treated mice compared to controls presented increased α-actin positive staining in the atherosclerotic plaque (**Figure 6B**). This is in line with increased collagen enrichment (Figure 4E, 4H) and the observation that TGFβ-1, a molecule with anti-atherogenic properties, emerged as a key increased upstream regulator following CX3CR1$^+$-Treg treatment (**Supplementary Figure 8A-8B**). ACT therapy with CX3CR1$^+$-Tregs also promoted the switch to a

more stable plaque as suggested by the downregulation of pathways associated with cellular infiltration, necrosis and apoptosis and the increase in pathways related to phagocytosis, including endocytosis, organization of actin cytoskeleton and LXR activation in the aorta of *Ldlr -/-* mice treated with CX3CR1^{+}-Treg compared to controls (**Figure 6C** and **Supplementary Figure 9A-9B**), suggesting a pro-resolutive polarization of local immune response. Of note, this immune switch was associated to a metabolic shift toward increased glycolysis and cholesterol efflux, but decreased oxygen consumption and oxidative metabolism coupled to reduced ATP synthesis in the aorta of *Ldlr -/-* treated with CX3CR1^{+}-Treg compared to mice treated with ctrl-Treg (**Figure 6D and Supplementary Figure 9C**). Although the levels of both macrophages and T lymphocytes (CD4 and CD8 T cells) were not different in the aorta of *Ldlr -/-* mice treated with CX3CR1^{+}-Treg (**Figure 6E-6F** and **Supplementary Figure 10A-10B)**, several modulators of efferocytosis were increased (MFGE8, LRP1 and calreticulin [5, 30-32]), while markers of decreased phagocytic ability -such as high mobility group box 1 (HMGB1)- were decreased (**Figure 6G** and **Supplementary Figure 11**) in the aorta of CX3CR1^{+}-Treg treated mice compared to *Ldlr -/-* treated with ctrl-Treg, thus confirming a shift toward a pro-resolutive specialized phagocytes following CX3CR1^{+}-Treg treatment. This response is further supported by the increased presence of apoptotic DNA fragments within macrophages supporting an increased presence of macrophages engulfing apoptotic cells, in the necrotic core of CX3CR1^{+} Treg treated mice compared to ctrl-Treg treated *Ldlr -/-* mice (**Figure 6H**), confirming overall an improved plaque phenotype following CX3CR1^{+} Treg treatment.

6. Discussion

Immune response in the vessels is finely tuned by the balance between inflammation and its resolution [5]; when this equilibrium is disrupted, as it occurs in the presence of hypercholesterolaemia, chronic inflammation prevails, thus favouring the atherogenic process [4]. This is in line with the chronic activation of the innate immune response reported in FH patients, where circulating monocytes [33] present a pro-inflammatory polarization. We have extended these findings showing that adaptive immune response is equally affected, not only in patients with asymptomatic carotid atherosclerosis [34], but also in FH patients, who presented an increased frequency of circulating effector memory $CD4^+$ T cells, of $CD4^+$ T cells proliferation rate and pro-inflammatory cytokine production compared to age- and sex-matched healthy controls. However, the reported observation that the pro-inflammatory activation persists in FH patients even after statin therapy [35], suggests that, parallel to lipid lowering therapies [36, 37], additional strategies should be considered to reduce the inflammatory burden and maximize the absolute cardiovascular benefit of FH patients . Of note, CANTOS study demonstrated that the inhibition of pro-inflammatory pathways such as IL-1β, protects from cardiovascular events independently of cholesterol lowering; treated patients, however, experienced increased risk of infection and fatal sepsis, thus suggesting the need for more tailored anti-inflammatory approaches. In this scenario, different strategies aimed at enhancing the immunosuppressive response have been tested in experimental models of atherosclerosis and among all, the promotion of Treg function appears to be particularly promising. However, despite convincing data from animal models, the association between Treg levels and atherosclerosis in humans is not univocal [11-15]. Here we correlated the increased inflammatory burden in FH patients to a decreased immunosuppressive response as suggested by reduced suppressive function of Tregs, an impairment that was compensated by increased circulating levels. Such a profile is common in several autoimmune diseases [28], including Sjögren syndrome and systemic lupus erythematosus disease [38, 39]. This leads to the concept that failure of Treg immunosuppressive activity contributes the pro-inflammatory response observed in FH patients and promotion of Treg activity would beneficially impact atherosclerosis disease. However this approach, although being effective in dampening disease progression, may either presented off-target immunosuppression due to systemic Treg increase or poor selectivity due to

the concomitant expansion of other immune cells [40] ; therefore, here we demonstrate that an approach able to hijack Tregs in the atherosclerotic plaque, would be beneficial for limiting disease-associated immuno-inflammation avoiding systemic immunosuppression.

To this aim we investigated a novel approach based on the possibility to target Tregs to the atherosclerotic plaque by inducing these cells to express chemokine receptors that match chemokines produced preferentially in the atherosclerotic lesion. The analysis of pro-inflammatory chemokines expressed during atherogenesis in *Ldlr -/-* mice revealed that both CCL2 and CX3CL1 were increased in the atherosclerotic plaque. However, although CCL2 has been widely associated to the atherogenic process [41], we detected an increased expression not only in the aorta, but also in lymphoid tissues and liver, thus limiting the possibility to exploit CCR2-CCL2 axis to drive cells to the atherosclerotic plaque. Vice versa, CX3CL1 showed a preferential expression in the aorta, but not in other tissues, pointing to an athero-selectivity of this axis. Both CX3CL1 and its counter-receptor (CX3CR1) have been shown to be upregulated in atherosclerotic lesion [42-44], and particularly in vulnerable plaques [45], while no expression of either the chemokine or its receptor has been detected in normal coronary arteries. Moreover, we showed that circulating levels of the cleaved form of CX3CL1 were increased in *Ldlr -/-* mice, in line with what was previously reported in patients with both stable and unstable angina pectoris [46]. Indeed, the CX3CL1/CX3CR1 axis participates in several pathological processes during atherogenesis including monocyte recruitment [47], and smooth muscle cell proliferation [48]. CX3CL1 KO models showed reduced atherosclerosis and the same was observed with pharmacological inhibition of CX3CL1 [49]. In humans, CX3CR1 expression on circulating leukocytes was shown to be increased in patients with coronary artery diseases [45, 50], and we have demonstrated that carriers of a polymorphism on fractalkine receptor (CX3CR1), resulting in reduced function, presented decreased subclinical atherosclerosis [51].

CX3CR1 is therefore critical to support atherosclerotic plaque selective homing and to this aim we engineered *wild type* Treg to overexpress CX3CR1. CX3CR1^{+}-engineered Tregs, 24 hours after the injection, preferentially localized at the aortic arch of *Ldlr -/-* mice and remained detectable even 4 weeks later, an effect that could also be driven by the anti-apoptotic signalling mediated by CX3CR1-CX3CL1 interaction[52, 53], thus enhancing engineered Tregs survival that might explain the increase levels of CX3CR1+GFP+ cells even after one month

from injection. Persistence of CX3CR1^{+}-Treg was associated with reduced atherosclerosis progression and improved plaque stability. Of note this effect was unrelated to changes in plasma cholesterol and triglycerides or in circulating immune cell signature, thus pointing to a local effect of our strategy as compared to previous studies showing that systemic FoxP3^{+} Treg deficiency impaired VLDL and chylomicron remnant clearance thus driving atherogenesis [54]. Of note, detailed characterization of the atherosclerotic plaque revealed important differences in extracellular matrix proteins, including the activation of the TGFβ-1 pathway, associated to the stabilization of the atherosclerotic plaque [55], coupled to increased SMCs abundance, and increased collagen deposition in CX3CR1^{+}-Treg treated *Ldlr -/-* mice compared to mice treated with ctrl-Treg.

Parallel to this, we observed that cellular infiltration, apoptosis and necrosis were significantly decreased while phagocytosis was upregulated in CX3CR1^{+}-Treg treated *Ldlr -/-* mice suggesting a shift toward a pro-resolutive response of phagocytes that has been proposed to be one of the key mechanisms involved in the atheroprotective effect of Tregs [10]. The increase in macrophages engulfed with apoptotic bodies points to and could be the consequence of improved efferocytosis in the aorta of *Ldlr -/-* mice after CX3CR1^{+}-Treg treatment. This hypothesis is supported by proteomic data showing the upregulation of LXR pathway, that could depend on LAL-mediated hydrolysis of lipids derived from apoptotic cells [4, 56], coupled to the increase in MFGE8, LRP1 and calreticulin and the reduction in HMGB1 [57] expression.

In summary our study supports the feasibility of exploiting the expression of chemokines receptors as a strategy to vehiculate cells to the atherosclerotic plaque, similar to what reported for gut CCR9 and integrin-α4β7 receptors in the context of transplantation and autoimmune diseases [58] and more importantly indicates that adoptive cell transfer with vasculotropic Treg dampens atherosclerosis development and improves plaque stability.

7. Author contributions

Conceived and designed the experiments: FB, EM, ALC, MK, GDN

Performed the experiments: FB, EM, JN, MC, AM

Analyzed the data: FB, EM, JN, MK, GDN

Performed proteomic analysis: MS, GB

Recruited healthy and FH subjects: FP, VZ

Wrote the paper: FB, GDN

All authors gave their final approval to the manuscript.

8. Acknowledgements

The help from technicians of the proteomic facility of the University of Milan (OMICS) for sample LC-MS/MS processing is kindly acknowledged.

9. Funding

This work was supported by: Ministero della Salute [GR-2013-02355011 to MK and FB]; Fondazione Cariplo [2016-0852 to GDN and 2019-1560 to FB]; Telethon Foundation [GGP19146 to GDN]; Progetti di Rilevante Interesse Nazionale [PRIN 2017 K55HLC to GDN].

10. Conflict of interest

None declare

11. Data availability

The raw data underlying this article will be shared on reasonable request to the corresponding author.

12. References

1. Warden BA, Fazio S, Shapiro MD. Familial Hypercholesterolemia: Genes and Beyond. In: Feingold KR, Anawalt B, Boyce A, Chrousos G, Dungan K, Grossman A*, et al.*, eds. Endotext. South Dartmouth (MA), 2000.
2. Mytilinaiou M, Kyrou I, Khan M, Grammatopoulos DK, Randeva HS. Familial Hypercholesterolemia: New Horizons for Diagnosis and Effective Management. *Front Pharmacol* 2018;**9**:707.
3. Nordestgaard BG, Chapman MJ, Humphries SE, Ginsberg HN, Masana L, Descamps OS, Wiklund O, Hegele RA, Raal FJ, Defesche JC, Wiegman A, Santos RD, Watts GF, Parhofer KG, Hovingh GK, Kovanen PT, Boileau C, Averna M, Boren J, Bruckert E, Catapano AL, Kuivenhoven JA, Pajukanta P, Ray K, Stalenhoef AF, Stroes E, Taskinen MR, Tybjaerg-Hansen A, European Atherosclerosis Society Consensus P. Familial hypercholesterolaemia is underdiagnosed and undertreated in the general population: guidance for clinicians to prevent coronary heart disease: consensus statement of the European Atherosclerosis Society. *Eur Heart J* 2013;**34**:3478-3490a.
4. Yvan-Charvet L, Bonacina F, Guinamard RR, Norata GD. Immunometabolic function of cholesterol in cardiovascular disease and beyond. *Cardiovasc Res* 2019;**115**:1393-1407.
5. Back M, Yurdagul A, Jr., Tabas I, Oorni K, Kovanen PT. Inflammation and its resolution in atherosclerosis: mediators and therapeutic opportunities. *Nat Rev Cardiol* 2019;**16**:389-406.
6. Gagliani N, Amezcua Vesely MC, Iseppon A, Brockmann L, Xu H, Palm NW, de Zoete MR, Licona-Limon P, Paiva RS, Ching T, Weaver C, Zi X, Pan X, Fan R, Garmire LX, Cotton MJ, Drier Y, Bernstein B, Geginat J, Stockinger B, Esplugues E, Huber S, Flavell RA. Th17 cells transdifferentiate into regulatory T cells during resolution of inflammation. *Nature* 2015;**523**:221-225.
7. Spitz C, Winkels H, Burger C, Weber C, Lutgens E, Hansson GK, Gerdes N. Regulatory T cells in atherosclerosis: critical immune regulatory function and therapeutic potential. *Cell Mol Life Sci* 2016;**73**:901-922.
8. Ou HX, Guo BB, Liu Q, Li YK, Yang Z, Feng WJ, Mo ZC. Regulatory T cells as a new therapeutic target for atherosclerosis. *Acta Pharmacol Sin* 2018;**39**:1249-1258.
9. Foks AC, Lichtman AH, Kuiper J. Treating atherosclerosis with regulatory T cells. *Arterioscler Thromb Vasc Biol* 2015;**35**:280-287.
10. Proto JD, Doran AC, Gusarova G, Yurdagul A, Jr., Sozen E, Subramanian M, Islam MN, Rymond CC, Du J, Hook J, Kuriakose G, Bhattacharya J, Tabas I. Regulatory T Cells Promote Macrophage Efferocytosis during Inflammation Resolution. *Immunity* 2018;**49**:666-677 e666.
11. Mailer RKW, Gistera A, Polyzos KA, Ketelhuth DFJ, Hansson GK. Hypercholesterolemia Enhances T Cell Receptor Signaling and Increases the Regulatory T Cell Population. *Sci Rep* 2017;**7**:15655.
12. Garetto S, Trovato AE, Lleo A, Sala F, Martini E, Betz AG, Norata GD, Invernizzi P, Kallikourdis M. Peak inflammation in atherosclerosis, primary biliary cirrhosis and autoimmune arthritis is counter-intuitively associated with regulatory T cell enrichment. *Immunobiology* 2015;**220**:1025-1029.
13. Ammirati E, Cianflone D, Banfi M, Vecchio V, Palini A, De Metrio M, Marenzi G, Panciroli C, Tumminello G, Anzuini A, Palloshi A, Grigore L, Garlaschelli K, Tramontana S, Tavano D, Airoldi F, Manfredi AA, Catapano AL, Norata GD. Circulating CD4+CD25hiCD127lo regulatory T-Cell levels do not reflect the extent or severity of carotid and coronary atherosclerosis. *Arterioscler Thromb Vasc Biol* 2010;**30**:1832-1841.
14. Zhu ZF, Meng K, Zhong YC, Qi L, Mao XB, Yu KW, Zhang W, Zhu PF, Ren ZP, Wu BW, Ji QW, Wang X, Zeng QT. Impaired circulating CD4+ LAP+ regulatory T cells in patients with acute coronary syndrome and its mechanistic study. *PloS one* 2014;**9**:e88775.
15. Dietel B, Cicha I, Voskens CJ, Verhoeven E, Achenbach S, Garlichs CD. Decreased numbers of regulatory T cells are associated with human atherosclerotic lesion vulnerability and inversely correlate with infiltrated mature dendritic cells. *Atherosclerosis* 2013;**230**:92-99.
16. Mallat Z, Gojova A, Brun V, Esposito B, Fournier N, Cottrez F, Tedgui A, Groux H. Induction of a regulatory T cell type 1 response reduces the development of atherosclerosis in apolipoprotein E-knockout mice. *Circulation* 2003;**108**:1232-1237.

17. Mor A, Planer D, Luboshits G, Afek A, Metzger S, Chajek-Shaul T, Keren G, George J. Role of naturally occurring CD4+ CD25+ regulatory T cells in experimental atherosclerosis. *Arterioscler Thromb Vasc Biol* 2007;**27**:893-900.
18. Dinh TN, Kyaw TS, Kanellakis P, To K, Tipping P, Toh BH, Bobik A, Agrotis A. Cytokine therapy with interleukin-2/anti-interleukin-2 monoclonal antibody complexes expands CD4+CD25+Foxp3+ regulatory T cells and attenuates development and progression of atherosclerosis. *Circulation* 2012;**126**:1256-1266.
19. Habets KL, van Puijvelde GH, van Duivenvoorde LM, van Wanrooij EJ, de Vos P, Tervaert JW, van Berkel TJ, Toes RE, Kuiper J. Vaccination using oxidized low-density lipoprotein-pulsed dendritic cells reduces atherosclerosis in LDL receptor-deficient mice. *Cardiovasc Res* 2010;**85**:622-630.
20. Hermansson A, Johansson DK, Ketelhuth DF, Andersson J, Zhou X, Hansson GK. Immunotherapy with tolerogenic apolipoprotein B-100-loaded dendritic cells attenuates atherosclerosis in hypercholesterolemic mice. *Circulation* 2011;**123**:1083-1091.
21. Klingenberg R, Lebens M, Hermansson A, Fredrikson GN, Strodthoff D, Rudling M, Ketelhuth DF, Gerdes N, Holmgren J, Nilsson J, Hansson GK. Intranasal immunization with an apolipoprotein B-100 fusion protein induces antigen-specific regulatory T cells and reduces atherosclerosis. *Arterioscler Thromb Vasc Biol* 2010;**30**:946-952.
22. Chyu KY, Dimayuga PC, Shah PK. Vaccine against arteriosclerosis: an update. *Ther Adv Vaccines* 2017;**5**:39-47.
23. Amirfakhryan H. Vaccination against atherosclerosis: An overview. *Hellenic J Cardiol* 2019.
24. Garetto S, Sardi C, Martini E, Roselli G, Morone D, Angioni R, Cianciotti BC, Trovato AE, Franchina DG, Castino GF, Vignali D, Erreni M, Marchesi F, Rumio C, Kallikourdis M. Tailored chemokine receptor modification improves homing of adoptive therapy T cells in a spontaneous tumor model. *Oncotarget* 2016;**7**:43010-43026.
25. Vignali D, Kallikourdis M. Improving homing in T cell therapy. *Cytokine Growth Factor Rev* 2017;**36**:107-116.
26. Casula M, Olmastroni E, Pirillo A, Catapano AL, Members Of The Lipigen Steering C, center PIC, Participant C, Participant L, Collaborators, Study Central L, Analysis G. Evaluation of the performance of Dutch Lipid Clinic Network score in an Italian FH population: The LIPIGEN study. *Atherosclerosis* 2018;**277**:413-418.
27. Bonacina F, Coe D, Wang G, Longhi MP, Baragetti A, Moregola A, Garlaschelli K, Uboldi P, Pellegatta F, Grigore L, Da Dalt L, Annoni A, Gregori S, Xiao Q, Caruso D, Mitro N, Catapano AL, Marelli-Berg FM, Norata GD. Myeloid apolipoprotein E controls dendritic cell antigen presentation and T cell activation. *Nature communications* 2018;**9**:3083.
28. Dominguez-Villar M, Hafler DA. Regulatory T cells in autoimmune disease. *Nature immunology* 2018;**19**:665-673.
29. Kallikourdis M, Andersen KG, Welch KA, Betz AG. Alloantigen-enhanced accumulation of CCR5+ 'effector' regulatory T cells in the gravid uterus. *Proceedings of the National Academy of Sciences of the United States of America* 2007;**104**:594-599.
30. Ait-Oufella H, Kinugawa K, Zoll J, Simon T, Boddaert J, Heeneman S, Blanc-Brude O, Barateau V, Potteaux S, Merval R, Esposito B, Teissier E, Daemen MJ, Leseche G, Boulanger C, Tedgui A, Mallat Z. Lactadherin deficiency leads to apoptotic cell accumulation and accelerated atherosclerosis in mice. *Circulation* 2007;**115**:2168-2177.
31. Yancey PG, Blakemore J, Ding L, Fan D, Overton CD, Zhang Y, Linton MF, Fazio S. Macrophage LRP-1 controls plaque cellularity by regulating efferocytosis and Akt activation. *Arterioscler Thromb Vasc Biol* 2010;**30**:787-795.
32. Gardai SJ, McPhillips KA, Frasch SC, Janssen WJ, Starefeldt A, Murphy-Ullrich JE, Bratton DL, Oldenborg PA, Michalak M, Henson PM. Cell-surface calreticulin initiates clearance of viable or apoptotic cells through trans-activation of LRP on the phagocyte. *Cell* 2005;**123**:321-334.
33. Bernelot Moens SJ, Neele AE, Kroon J, van der Valk FM, Van den Bossche J, Hoeksema MA, Hoogeveen RM, Schnitzler JG, Baccara-Dinet MT, Manvelian G, de Winther MPJ, Stroes ESG. PCSK9

monoclonal antibodies reverse the pro-inflammatory profile of monocytes in familial hypercholesterolaemia. *Eur Heart J* 2017;**38**:1584-1593.
34. Ammirati E, Cianflone D, Vecchio V, Banfi M, Vermi AC, De Metrio M, Grigore L, Pellegatta F, Pirillo A, Garlaschelli K, Manfredi AA, Catapano AL, Maseri A, Palini AG, Norata GD. Effector Memory T cells Are Associated With Atherosclerosis in Humans and Animal Models. *J Am Heart Assoc* 2012;**1**:27-41.
35. Bekkering S, Stiekema LCA, Bernelot Moens S, Verweij SL, Novakovic B, Prange K, Versloot M, Roeters van Lennep JE, Stunnenberg H, de Winther M, Stroes ESG, Joosten LAB, Netea MG, Riksen NP. Treatment with Statins Does Not Revert Trained Immunity in Patients with Familial Hypercholesterolemia. *Cell Metab* 2019;**30**:1-2.
36. Catapano AL, Pirillo A, Norata GD. Anti-PCSK9 antibodies for the treatment of heterozygous familial hypercholesterolemia: patient selection and perspectives. *Vasc Health Risk Manag* 2017;**13**:343-351.
37. Norata GD, Ballantyne CM, Catapano AL. New therapeutic principles in dyslipidaemia: focus on LDL and Lp(a) lowering drugs. *Eur Heart J* 2013;**34**:1783-1789.
38. Alunno A, Petrillo MG, Nocentini G, Bistoni O, Bartoloni E, Caterbi S, Bianchini R, Baldini C, Nicoletti I, Riccardi C, Gerli R. Characterization of a new regulatory CD4+ T cell subset in primary Sjogren's syndrome. *Rheumatology (Oxford)* 2013;**52**:1387-1396.
39. Ferreira RC, Castro Dopico X, Oliveira JJ, Rainbow DB, Yang JH, Trzupek D, Todd SA, McNeill M, Steri M, Orru V, Fiorillo E, Crouch DJM, Pekalski ML, Cucca F, Tree TI, Vyse TJ, Wicker LS, Todd JA. Chronic Immune Activation in Systemic Lupus Erythematosus and the Autoimmune PTPN22 Trp(620) Risk Allele Drive the Expansion of FOXP3(+) Regulatory T Cells and PD-1 Expression. *Front Immunol* 2019;**10**:2606.
40. Tomala J, Chmelova H, Mrkvan T, Rihova B, Kovar M. In vivo expansion of activated naive CD8+ T cells and NK cells driven by complexes of IL-2 and anti-IL-2 monoclonal antibody as novel approach of cancer immunotherapy. *J Immunol* 2009;**183**:4904-4912.
41. Aiello RJ, Bourassa PA, Lindsey S, Weng W, Natoli E, Rollins BJ, Milos PM. Monocyte chemoattractant protein-1 accelerates atherosclerosis in apolipoprotein E-deficient mice. *Arterioscler Thromb Vasc Biol* 1999;**19**:1518-1525.
42. Umehara H, Bloom E, Okazaki T, Domae N, Imai T. Fractalkine and vascular injury. *Trends Immunol* 2001;**22**:602-607.
43. Wong BW, Wong D, McManus BM. Characterization of fractalkine (CX3CL1) and CX3CR1 in human coronary arteries with native atherosclerosis, diabetes mellitus, and transplant vascular disease. *Cardiovasc Pathol* 2002;**11**:332-338.
44. Combadiere C, Potteaux S, Gao JL, Esposito B, Casanova S, Lee EJ, Debre P, Tedgui A, Murphy PM, Mallat Z. Decreased atherosclerotic lesion formation in CX3CR1/apolipoprotein E double knockout mice. *Circulation* 2003;**107**:1009-1016.
45. Zhang X, Feng X, Cai W, Liu T, Liang Z, Sun Y, Yan C, Han Y. Chemokine CX3CL1 and its receptor CX3CR1 are associated with human atherosclerotic lesion volnerability. *Thrombosis research* 2015;**135**:1147-1153.
46. Ikejima H, Imanishi T, Tsujioka H, Kashiwagi M, Kuroi A, Tanimoto T, Kitabata H, Ishibashi K, Komukai K, Takeshita T, Akasaka T. Upregulation of fractalkine and its receptor, CX3CR1, is associated with coronary plaque rupture in patients with unstable angina pectoris. *Circ J* 2010;**74**:337-345.
47. Stolla M, Pelisek J, von Bruhl ML, Schafer A, Barocke V, Heider P, Lorenz M, Tirniceriu A, Steinhart A, Bauersachs J, Bray PF, Massberg S, Schulz C. Fractalkine is expressed in early and advanced atherosclerotic lesions and supports monocyte recruitment via CX3CR1. *PloS one* 2012;**7**:e43572.
48. Liu H, Jiang D. Fractalkine/CX3CR1 and atherosclerosis. *Clin Chim Acta* 2011;**412**:1180-1186.
49. Poupel L, Boissonnas A, Hermand P, Dorgham K, Guyon E, Auvynet C, Charles FS, Lesnik P, Deterre P, Combadiere C. Pharmacological inhibition of the chemokine receptor, CX3CR1, reduces atherosclerosis in mice. *Arterioscler Thromb Vasc Biol* 2013;**33**:2297-2305.

50. Damas JK, Boullier A, Waehre T, Smith C, Sandberg WJ, Green S, Aukrust P, Quehenberger O. Expression of fractalkine (CX3CL1) and its receptor, CX3CR1, is elevated in coronary artery disease and is reduced during statin therapy. *Arterioscler Thromb Vasc Biol* 2005;**25**:2567-2572.
51. Norata GD, Garlaschelli K, Ongari M, Raselli S, Grigore L, Catapano AL. Effects of fractalkine receptor variants on common carotid artery intima-media thickness. *Stroke* 2006;**37**:1558-1561.
52. White GE, McNeill E, Channon KM, Greaves DR. Fractalkine promotes human monocyte survival via a reduction in oxidative stress. *Arterioscler Thromb Vasc Biol* 2014;**34**:2554-2562.
53. White GE, Tan TC, John AE, Whatling C, McPheat WL, Greaves DR. Fractalkine has anti-apoptotic and proliferative effects on human vascular smooth muscle cells via epidermal growth factor receptor signalling. *Cardiovasc Res* 2010;**85**:825-835.
54. Klingenberg R, Gerdes N, Badeau RM, Gistera A, Strodthoff D, Ketelhuth DF, Lundberg AM, Rudling M, Nilsson SK, Olivecrona G, Zoller S, Lohmann C, Luscher TF, Jauhiainen M, Sparwasser T, Hansson GK. Depletion of FOXP3+ regulatory T cells promotes hypercholesterolemia and atherosclerosis. *J Clin Invest* 2013;**123**:1323-1334.
55. Frutkin AD, Otsuka G, Stempien-Otero A, Sesti C, Du L, Jaffe M, Dichek HL, Pennington CJ, Edwards DR, Nieves-Cintron M, Minter D, Preusch M, Hu JH, Marie JC, Dichek DA. TGF-[beta]1 limits plaque growth, stabilizes plaque structure, and prevents aortic dilation in apolipoprotein E-null mice. *Arterioscler Thromb Vasc Biol* 2009;**29**:1251-1257.
56. Gomaraschi M, Bonacina F, Norata GD. Lysosomal Acid Lipase: From Cellular Lipid Handler to Immunometabolic Target. *Trends in pharmacological sciences* 2019;**40**:104-115.
57. Banerjee S, de Freitas A, Friggeri A, Zmijewski JW, Liu G, Abraham E. Intracellular HMGB1 negatively regulates efferocytosis. *J Immunol* 2011;**187**:4686-4694.
58. Romano M, Fanelli G, Albany CJ, Giganti G, Lombardi G. Past, Present, and Future of Regulatory T Cell Therapy in Transplantation and Autoimmunity. *Front Immunol* 2019;**10**:43.

13. Figure Legends

Figure 1. Severe hypercholesterolemia is associated with impaired Treg immunosuppressive response.

A) Levels of circulating CD4+ Teffector memory ($CCR7^{-}CD45RA^{-}$; p=0.033), Tcentral memory ($CCR7^{+}CD45RA^{-}$; p=0.0009) and Tnaive cells ($CCR7^{+}CD45RA^{+}$) in subjects affected by familial hypercholesterolemia (FH, He for LDLR mutation) and age- and sex- matched healthy controls (n=51 for ctrl and n=48 for FH); representative density plots from flow cytometric analysis showing the distribution of CD4 subsets gated on lymphocytes $CD4^{+}$ are presented. B) Proliferation of CD4 T cells in FH compared to healthy controls after in vitro activation with anti-CD3/28 + IL-2 for 5 days (mitotic index is presented, see supplemental methods for details. N=15/group; p=0.0025); representative histograms of CFSE dilution from flow cytometric analysis showing picks of subsequent division of cells are presented (each colour represents a generation of divided cells). C) Production of pro-inflammatory (TNFα, IFNγ) and anti-inflammatory (IL-10) cytokines in CD4+ T cells from FH patients compared to healthy controls under resting conditions and after in vitro activation with anti-CD3/28 + IL-2 for 5 days (n=15/group; p=0.014 for IFNγ and p=0.029 for IL-10). D) Levels of circulating Tregulatory cells (Treg, $CD4^{+}CD127^{lo}CD25^{hi}$) in FH patients compared to age- and sex- matched healthy controls (n=59/group; p=0.0016); representative density plots from flow cytometric analysis showing Treg cell gatings are presented. E) Suppression of CD4 T conventional ($CD4^{+}CD25^{-}$) proliferation by autologous Treg ($CD4^{+}CD25^{+}$) in FH patients compared to healthy controls (n=5/group; p=0.034, p=0.027 , p=0.003 respectively for conditions 1:0.25, 1:0.5 and 1:1 Tconv:Treg); quantification of the area under the curves (AUC) of CD4 proliferation is presented in the right inside panel. Statistical analysis was performed with unpaired Ttest; data are reported as mean ± SEM; *p<0.05, **p<0.01.

Figure 2. CX3CR1/CX3CL1 axis confers atherosclerotic plaque selectivity.

A) Heatmap from mRNA expression of a set of inflammatory cytokines (CCL2, CCL5, CCL4, CXCL9, CXCL10, CXCL11 and CX3CL1) in the aorta, mediastinal (heart-draining) and inguinal lymph nodes, spleen and liver of *wild type* and *Ldlr -/-* mice after 8 weeks of high-cholesterol (western type) diet (n=3/group), normalized on *wild type* expression in spleen. B) mRNA expression of CX3CL1 in the aorta, mediastinal (heart-draining) and

inguinal lymph nodes, spleen and liver of *wild type* and *Ldlr -/-* mice after 8 weeks of high-cholesterol diet (n=3/group; P=0.001) normalized on *wild type* expression in spleen. C) CX3CL1 plasma concentration in *wild type* and *Ldlr -/-* mice (n=3/group; mean of triplicates; p=8.0 x 10^{-7}). D) expression of CX3CR1 on $CD4^+$ T cells and $Ly6C^+$ monocytes in *wild type* mice (n=4/group; p=6.08 x 10^{-5}); representative histograms of CX3CR1 expression in CD4 Tcells and monocytes compared to negative staining (fluorescence minus one, FMO) are shown. Statistical analysis was performed with two-way anova multiple comparison test comparing the mean of mRNA expression in *wild type* versus *Ldlr -/-* for each tissue with Sidak correction (B); and with unpaired Ttest (C, D); data are reported as mean ± SEM; **p<0.01.

Figure 3. Engineered Tregs overexpressing CX3CR1 home preferentially to the atherosclerotic plaque.

A) Schematic representation of the workflow of *wild type* Treg isolation and transduction (empty vector: GFP^+ ctrl-Treg; CX3CR1-IRES-EGFP vector: GFP^+ CX3CR1-Treg) and Treg adoptive cell therapy (ACT) in LDLR KO. Isolated and transduced Tregs from *wild type* mice were injected ($2x10^5$ cells) in *Ldlr -/-* mice after 8 weeks of high-cholesterol diet (WTD). 24 hours after the injection mice were sacrificed for analysis of Treg homing. B) CX3CR1 expression in transduced Tregs by flow cytometry. C) Levels of GFP^+ cells out of $CD45^+$ live cells in the aorta of 8-week WTD *Ldlr -/-* mice 24 hours after the injection of $2x10^5$ Ctrl- or $CX3CR1^+$-Treg by flow cytometry (n=4 for ctrl-Treg and n=5 for $CX3CR1^+$-Treg; p=0,023). Representative dot plots from flow cytometry analysis are shown. Statistical analysis was performed with unpaired Ttest; data are reported as mean ± SEM; *p<0.05.

Figure 4. $CX3CR1^+$ Tregs dampen atherosclerosis progression.

A) Schematic representation of the protocol of ACT with engineered Tregs in *Ldlr -/-* mice (drawn with Biorender software). 4 weeks after ACT atherosclerosis progression was evaluated. B) Frequency of GFP^+ cells (engineered Treg) in the atherosclerotic plaque of *Ldlr -/-* mice (n=5/group, p=0.05). C) Atherosclerotic plaque area (expressed in μm^2; n=8/group, p=0.038), D) necrotic core (expressed in μm^2; n=8/group), E) collagen content (Masson's trichrome staining expressed as % of positive stained area (blue staining) compared to total plaque area (n=11/group, p=0.026), and F) lipid content (oil red'O staining expressed as % of positive stained area (red staining) compared to total plaque area (n=10/group, p=0.014)) at the aortic sinus of *Ldlr -/-* mice, 4

weeks after Treg ACT. G) Representative pictures of haematoxylin and eosin, Masson's trichrome and oil red'O staining at the aortic sinus (magnification 5x, scale bar 200 μm). Statistical analyses were performed with unpaired Ttest; data are reported as mean ± SEM; *p<0,05.

Figure 5. Proteomic analysis of aorta from *Ldlr -/-* mice treated with ctrl- or CX3CR1^{+}-Treg

A) Volcano plot showing the log2 fold-change (x-axis) against the –log10 statistical p value (y-axis) of proteomic data from aorta of *Ldlr -/-* mice treated with ctrl-Treg or CX3CR1^{+}-Treg. Increased proteins are marked in red (p<0.05, FC>1.5), while those decreased are marked in blue (p<0.05, FC<-1.5) of three technical replicates derived from respectively 4 and 5 aorta of ctrl- and CX3CR1^{+}-Treg treated *Ldlr -/-*. B) Principal component analysis (PCA) of proteomic data from aorta of *Ldlr -/-* mice treated with ctrl-Treg or CX3CR1^{+}-Treg, each point represents a technical replicate. C) Heatmap with hierarchical clustering based on Pearson correlation showing LFQ protein intensities of 342 significant proteins (p<0.05, FDR<0.05). D) Biological network analysis of the main pathways (FDR<0.05) for the significant proteins (p-value<0.05), generated by Cytoscape software with plug-ins StringApp, Reactome and KEGG, genes noted with red are upregulated, while with blue are down-regulated in CX3CR1^{+}-Treg compared to Ctrl-Treg treatment.

Figure 6. Engineered Tregs dampen immune response in the atherosclerotic plaque

A) z-score analysis of pathways associated to extracellular matrix organization processed by IPA software. B) Smooth muscle cell content (α-actin staining) in atherosclerotic plaque from *Ldlr -/-* mice treated with ctrl-Treg or CX3CR1+-Treg. Data are expressed as % of α-actin positive stained area compared to total plaque area (n=5/group, p=0.047); representative pictures of α-actin staining at the aortic sinus (α-actin positive cells in red, DAPI in blue; magnification 10x, scale bar 50 μm). C) z-score analysis and of pathways associated to metabolism and D) inflammation processed by IPA software. E) Frequency of macrophages in the aorta of *Ldlr -/-* mice treated with ctrl- or CX3CR1^{+}-Treg detected by flow cytometry (n=5/group). F) Immunofluorescent analysis of macrophages staining in the aortic plaque (Mac-2 positive cells in red, DAPI in blue; magnification 10x, scale bar 50 μm). G) Quantification of proteins associated to efferocytosis identified by proteomic analysis of aorta from *Ldlr -/-* mice isolated 4 weeks after Treg ACT with CX3CR1+- or ctrl-Treg (n=3 technical replicates;

p<0.05). H) Detection of apoptotic cells by TUNEL staining (green), macrophages (Mac-2; red) and nuclei (DAPI, blue); representative TUNEL positive signals are highlighted by white arrows (magnification 10x, scale bar 100 or 50 µm). Statistical analyses were performed with unpaired Ttest (B, F) or two-way anova multiple comparison test comparing protein abundance between CX3CR1+ and ctrl-Treg aorta with Sidak correction (G); data are reported as mean ± SEM; *p<0.05.

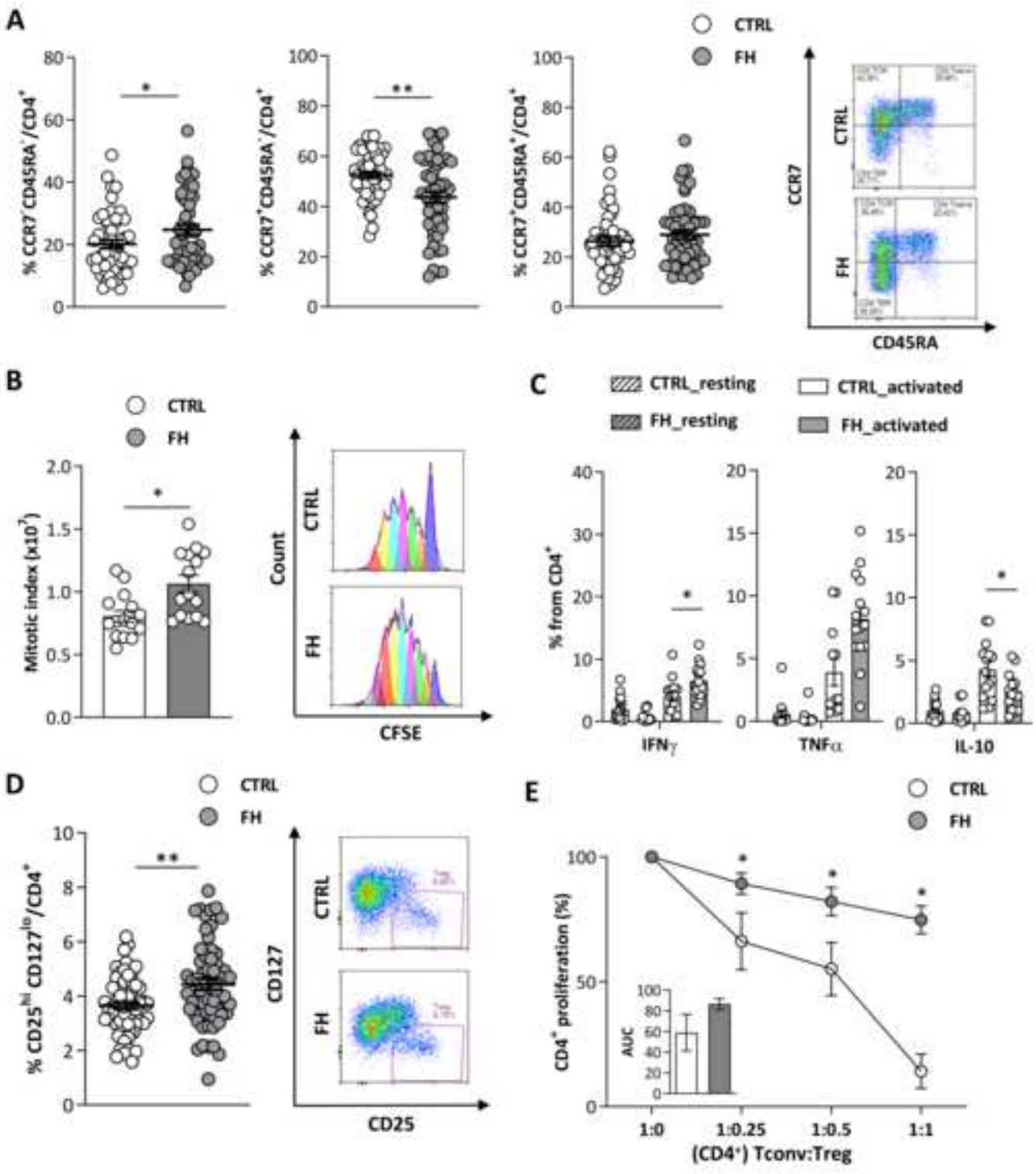

Figure 1

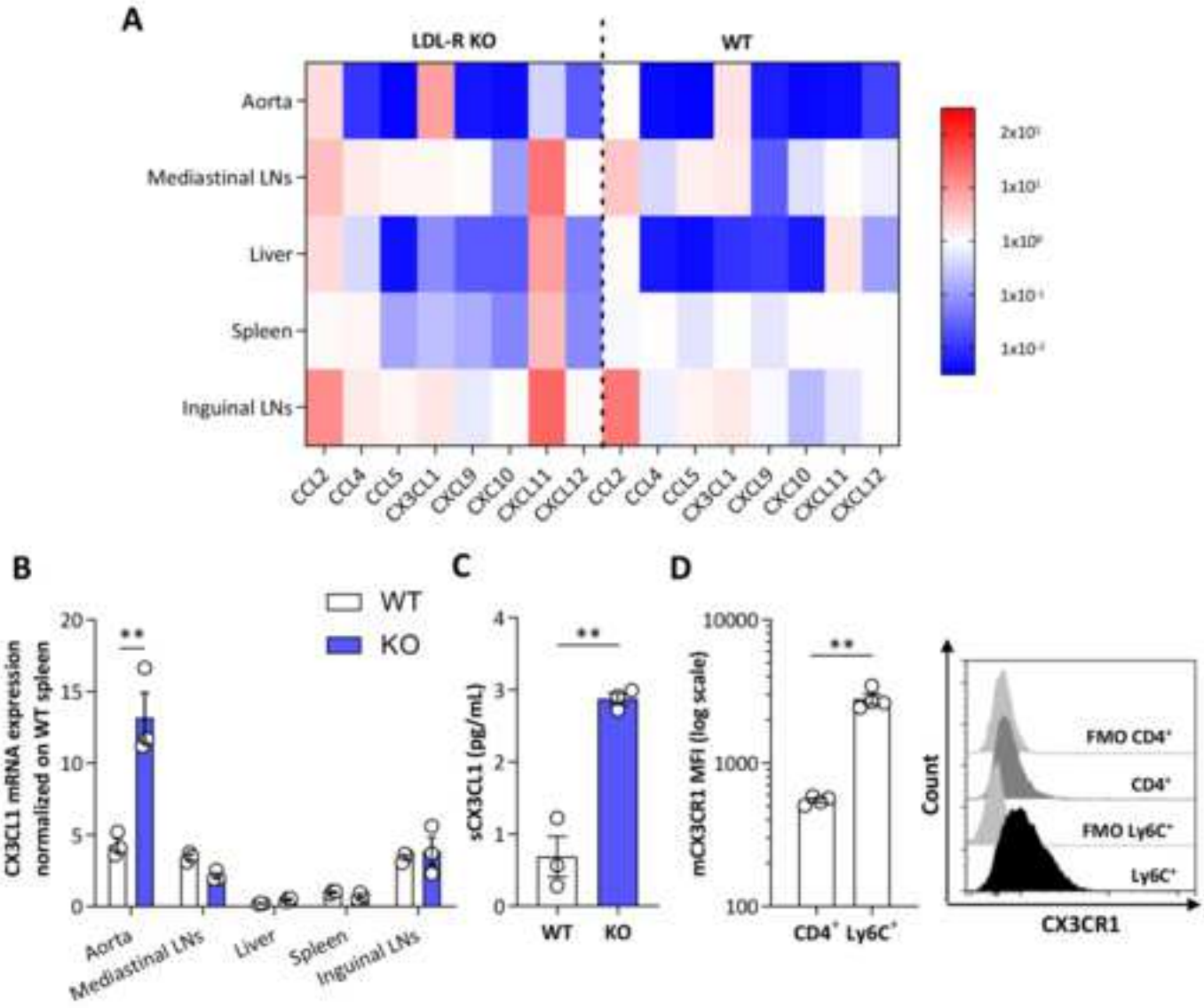

Figure 2

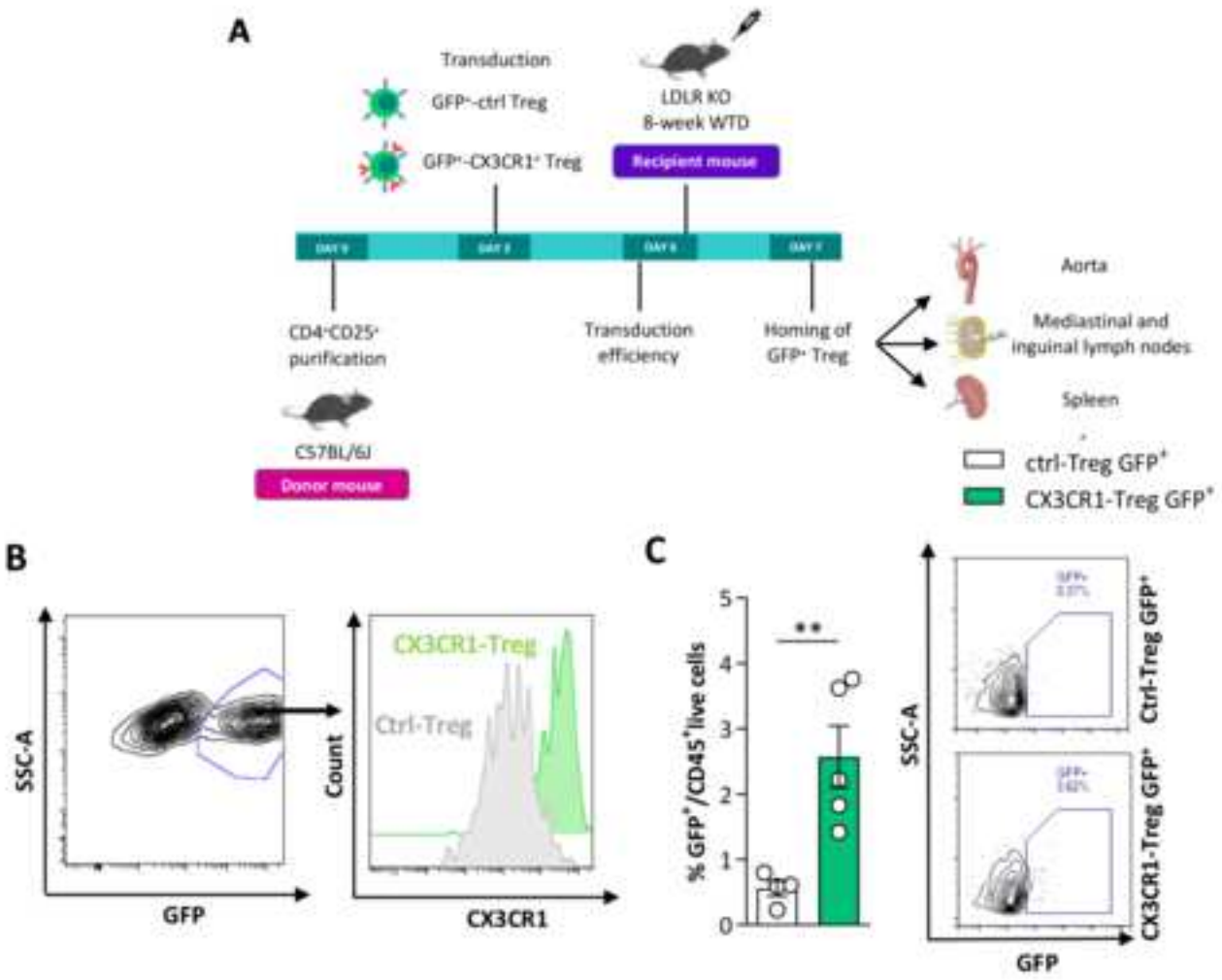

Figure 3

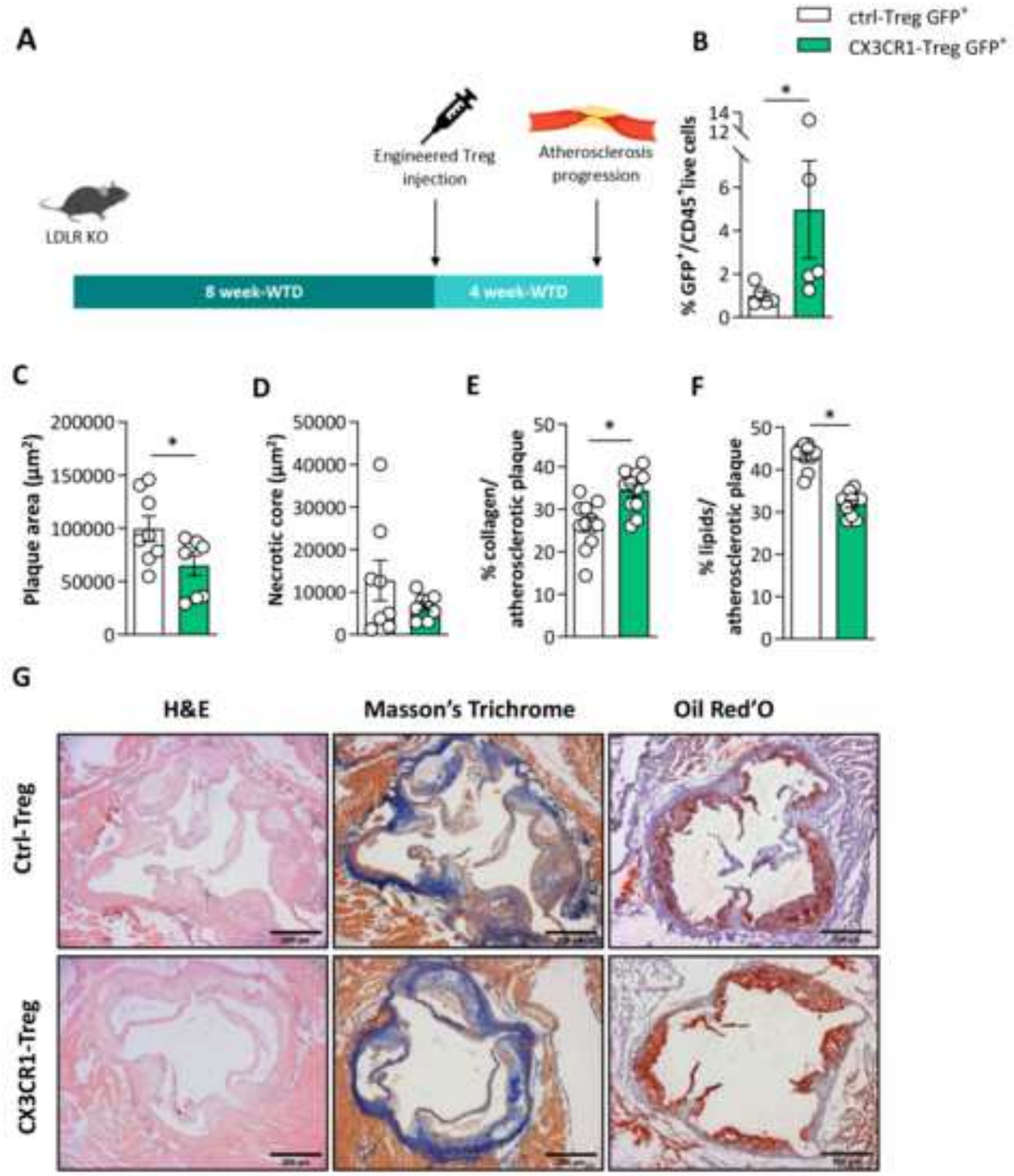

Figure 4

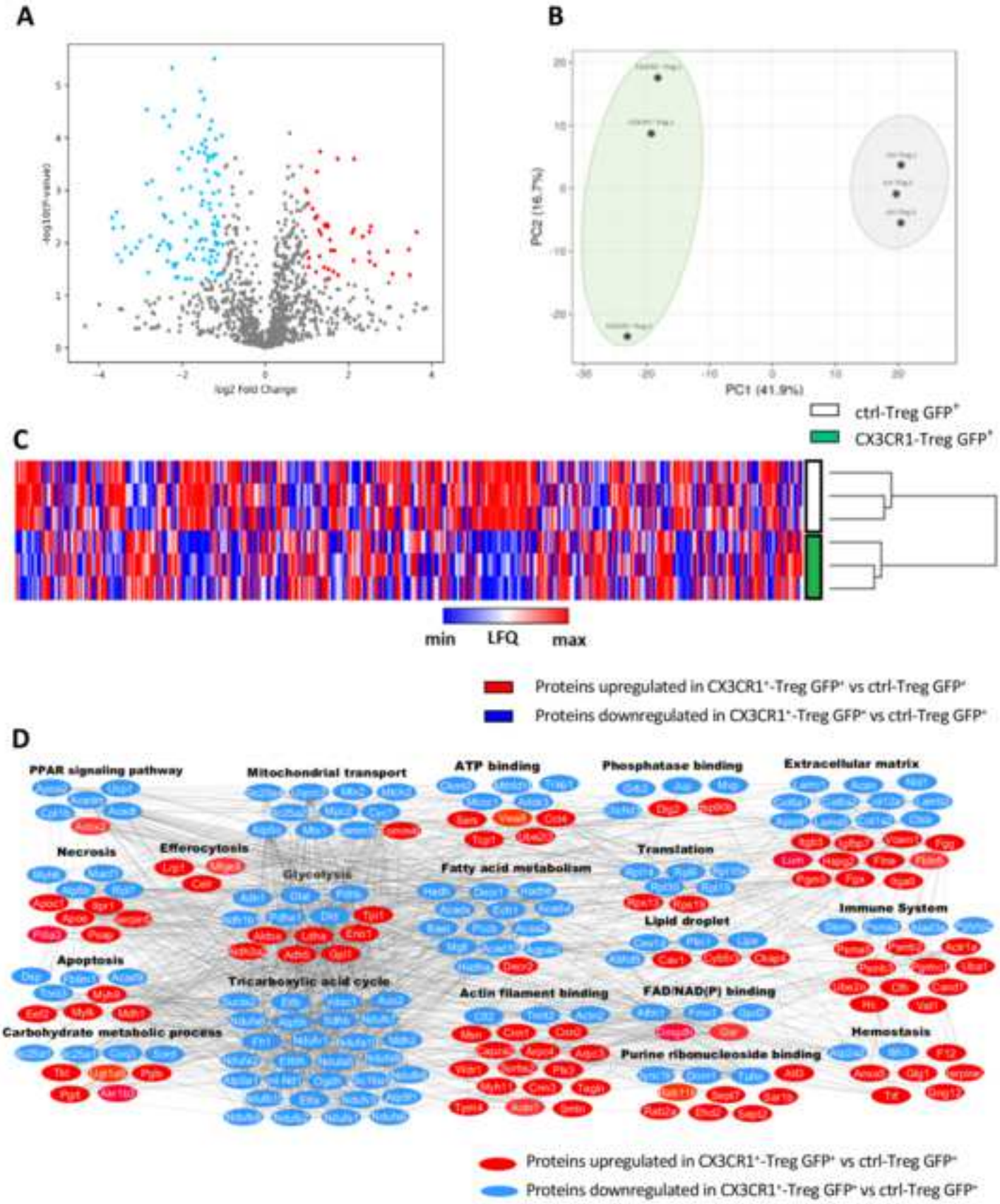

Figure 5

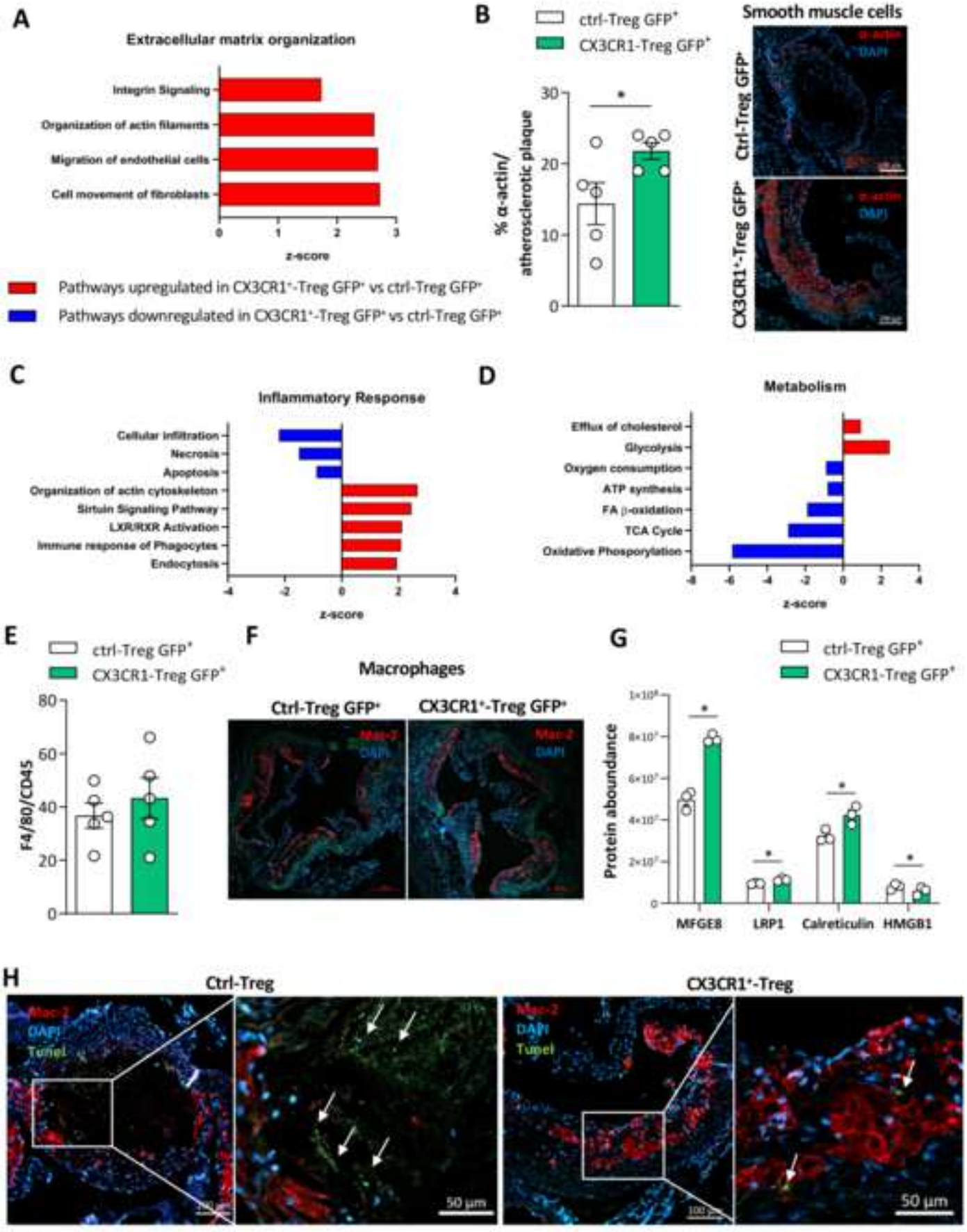

Figure 6.

Graphical Abstract